ACS Catalysis

RESEARCH ARTICLE

pubs.acs.org/acscatalysis

Quantification of Reactive CO and H_2 on CuO_x-CeO_2 during CO Preferential Oxidation by Reactive Titration and Steady State Isotopic Transient Kinetic Analysis

Rong Zhang, Tala Haddadin, Diana P. Rubiano, Hari Nair, Christopher S. Polster, and Chelsey D. Baertsch*

School of Chemical Engineering, Purdue University, 480 Stadium Mall Drive, West Lafayette, Indiana 47907, United States

ABSTRACT: The molar quantity of adsorbed CO and H_2 present on the surface of a mixed CuO_x-CeO_2 catalyst during CO preferential oxidation in H_2 at 353 K was quantified using both the reactive titration method and the steady-state isotopic-transient kinetic analysis (SSITKA). For the reactive titration method, either CO or H_2 was replaced by He during steady state reaction while monitoring the residual transient product formation of CO_2 or H_2O produced from the surface adsorbed CO or H_2 via catalytic oxidations. For SSITKA, ^{12}CO was replaced by ^{13}CO during steady state reaction while monitoring the transient product formation of $^{12}CO_2$. The amount of adsorbed reactive CO increases with increasing CO partial pressure or decreasing H_2 partial pressure, while the amount of reactive H_2 decreases with increasing CO partial pressure or decreasing H_2 partial pressure, showing that the adsorbed CO and H_2 compete for active redox sites and prohibit the other's adsorption. Using reactive CO and H_2 amounts, two models of coverage were defined with trends providing insight into the competitive redox mechanism between adsorbed CO and H_2. CO oxidation is kinetically preferred over CuO_x-CeO_2, and the relative CO to H_2 coverage is shown to be the determiner for CO_2 selectivity. This new depiction of selectivity parameters provides a useful principle for the design of selective PROX catalysts.

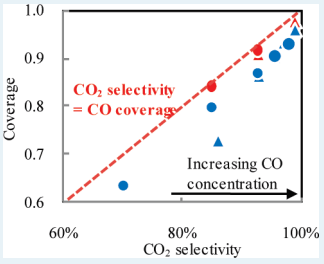

KEYWORDS: PROX, oxidation selectivity, active site quantification, reactive titration, isotope exchange, copper cerium oxide

1. INTRODUCTION

CO preferential oxidation (PROX) is used to purify reformed H_2 (often containing up to 1% CO) for use in CO-sensitive Proton Exchange Membrane (PEM) Fuel Cells.[1−5] Catalysts capable of high selectivity CO PROX also enable online catalytic detection and monitoring of CO (often below 100 ppm) after the H_2 purification step.[6] A high CO oxidation selectivity in the reactive mixture is preferred to minimize H_2 consumption during gas purification and to minimize a false sensor response from H_2 oxidation in an online microsensor. Mixed copper cerium oxide catalysts (CuO_x-CeO_2) are highly selective for the CO PROX reaction across a wide range of CO pressures, in contrast to Pt or Au based catalysts, which lose CO_2 selectivity at low CO pressures;[1,7−9] CuO_x-CeO_2 provides 100% CO_2 selectivity down to 200 ppm CO at 333 K.[6]

The loss of CO_2 selectivity with decreasing CO pressure results from the competitive mechanism between CO and H_2 over the same active redox site,[6,10] which is generally accepted as the interfacial sites between Cu and Ce in a mixed oxide structure.[11−18] The CO and H_2 competitive redox mechanism was proposed upon the inspection of H_2 addition effect during CO oxidation and vice versa,[19,20] and was supported by our previously reported kinetic model assuming Mars and van Krevelen reaction pathways.[10] On the basis of the competitive CO and H_2 redox mechanism, a higher CO coverage during reaction would lead to a higher CO_2 selectivity. Therefore, the goal of this paper is to quantify the amount of redox active CO and H_2 present on the surface of CuO_x-CeO_2 during PROX reactions of varying CO and H_2 pressures to provide further insight into the previously described competitive redox mechanism, and to describe the observed decrease in CO_2 selectivity with decreasing CO pressure.

Only a limited number of techniques can be used to quantify the amount of adsorbed CO and H_2 under reaction conditions.[21,22] Steady-state isotopic-transient kinetic analysis (SSITKA) has been used to measure reactant amounts under reaction conditions,[23−26] and is used here to probe the amounts of adsorbed CO and H_2 that are oxidized to redox products. Because of the economical concern of the expensive isotopic gas, a more cost-effective reactive titration method is also proposed and used for routine measurement of catalyst coverages. Using both methods, reactive coverages of CO and H_2 were quantified and used to develop a model relating variations in CO_2 selectivity to CO surface coverage under reaction conditions.

2. EXPERIMENTAL SECTION

2.1. Catalyst Preparation and Characterization. A copper cerium mixed metal oxide catalyst (CuO_x-CeO_2) was synthesized by the urea gelation technique and characterized by Brunauer−Emmett−Teller (BET) surface area measurements, X-ray diffraction (XRD), atomic absorption spectroscopy (AAS), and X-ray photoelectron spectroscopy (XPS), with methods and results reported previously.[6,10] The surface area of CuO_x-CeO_2 is

Received: January 22, 2011
Revised: March 12, 2011
Published: March 21, 2011

115.8 $m^2 g^{-1}$. The absence of any copper metal or copper oxide phases observed by XRD indicates that either Cu is doped into the CeO_2 lattice or present at the surface or the subsurface in small dispersed domains. The bulk Cu atomic content in CuO_x-CeO_2 from AAS is 4.5%, and the Ce/Cu surface atomic ratio from XPS is 7:1, indicating that some Cu is segregated to the CuO_x-CeO_2 surface.

2.2. Oxidation Reactions. All reactions were carried out in a vertical U-shaped continuous flow quartz reactor with a diameter of 10 mm and heated in a tube furnace. All reactions were carried out at less than 10% CO and H_2 conversion to approximate differential conditions. The reaction temperature was controlled by a thermocouple placed in a well above the catalyst bed. All catalyst samples were sieved to retain particles between 75 and 125 μm. Inert white quartz sand (SiO_2, −50 + 70 mesh; Sigma-Aldrich) was used to dilute the CuO_x-CeO_2 catalyst in a 1 to 10 mass ratio (excess sand) to avoid temperature gradients across the catalyst bed. The catalyst was pretreated in flowing O_2 (Praxair, 10% O_2/He, certified standard) at 773 K (20 K min^{-1} then 30 min soak) before cooling to the reaction temperature of 353 K. Subsequently, CO (Praxair, 1000 ppm CO/He, certified standard), H_2 (Praxair, 99.9999%), O_2 (Praxair, 1000 ppm O_2/He, certified standard), and makeup He (Praxair, 99.9999%) were introduced using calibrated mass flow controllers (Laminar Technologies, Tylan 2900 series). Reactions were carried out using 50−900 ppm CO, 25−450 ppm O_2, and 10−40% H_2. Reaction rates and CO_2 selectivity were obtained by analyzing the products (CO_2 and H_2O) using an Agilent MicroGC 3000 with Plot Q and molecular sieve columns. The CO rate was calculated by taking the ratio of the CO_2 production molar flow rate (mol s^{-1}) to the catalyst weight (g). Similarly, the H_2 rate was calculated by taking the ratio of the H_2O production molar flow rate (mol s^{-1}) to the catalyst weight (g). CO_2 selectivity was calculated as the CO_2 production rate divided by the sum of CO_2 and H_2O production rates.

2.3. Reactive Titration. After about 16 h of activation to reach steady state at 353 K, reactive titration experiments were carried out by instantaneously removing either CO or H_2 from the feed stream and adding makeup He using a four-port zero dead volume switching valve (Valco) to retain the same total flow rate (150 sccm). All gas species were monitored by a Hiden HPR 20 Gas Analyzer at m/z of 2 (H_2), 18 (H_2O), 28 (CO), 32 (O_2), and 44 (CO_2).

2.4. Steady-State Isotopic-Transient Kinetic Analysis (SSITKA). SSITKA was carried out by making an instantaneous switch from ^{12}CO to ^{13}CO (1% ^{13}CO, 1% Ar, 98% He, Cambridge Isotope Laboratories) using a four-port zero dead volume switching valve (Valco). The total flow rate was kept constant at 150 sccm. Once the concentration of all isotopes reached a steady-state level (about 10 min after the switch), the opposite switch from ^{13}CO to ^{12}CO was performed. All gas species were monitored at m/z of 2 (H_2), 18 (H_2O), 28 (^{12}CO), 29 (^{13}CO), 32 (O_2), 40 (Ar), 44 (CO_2), and 45 ($^{13}CO_2$).

3. RESULTS AND DISCUSSION

3.1. Effect of CO Pressure on CO Rate, H_2 Rate, and CO_2 Selectivity. Before examining surface coverages, details of the kinetics of CO and H_2 oxidation over CuO_x-CeO_2 are presented here at low CO pressures to describe key variations in selectivity at these conditions. Under CO PROX conditions, CO partial pressure in the reactant feed affects CO and H_2 oxidation rates as well as the CO_2 selectivity (Figure 1). As shown in Figure 1a, CO oxidation rates continuously increase with increasing CO pressure from 50 to 600 ppm. At any CO pressure, the CO rate in 10% H_2 is higher than that in 25% H_2, showing that the presence of H_2 reduces CO rates. On the basis of our previous study, this presumably results from competitive adsorption of CO and H_2 on the same active sites, by which the presence of more H_2 prohibits the adsorption of CO molecules, and hence reduces CO oxidation rates.[10] Similarly, an increase in CO pressure reduces H_2 rates at both H_2 pressures (Figure 1b), and at any CO pressure, the H_2 rate with 25% H_2 is higher than that with 10% H_2. CO and H_2 oxidation rates are interdependent on their relative concentrations in the gas phase, presumably as a result of changes in relative surface concentrations, which is examined further in this study. Since the CO rate increases and the H_2 rate decreases with increasing CO pressure, the CO_2 selectivity also increases with increasing CO pressure, as shown in Figure 1c. The CO_2 selectivity in 10% H_2 is consistently higher than that in 25% H_2, and at 600 ppm CO, the CO_2 selectivity reaches 100% in 10% H_2.

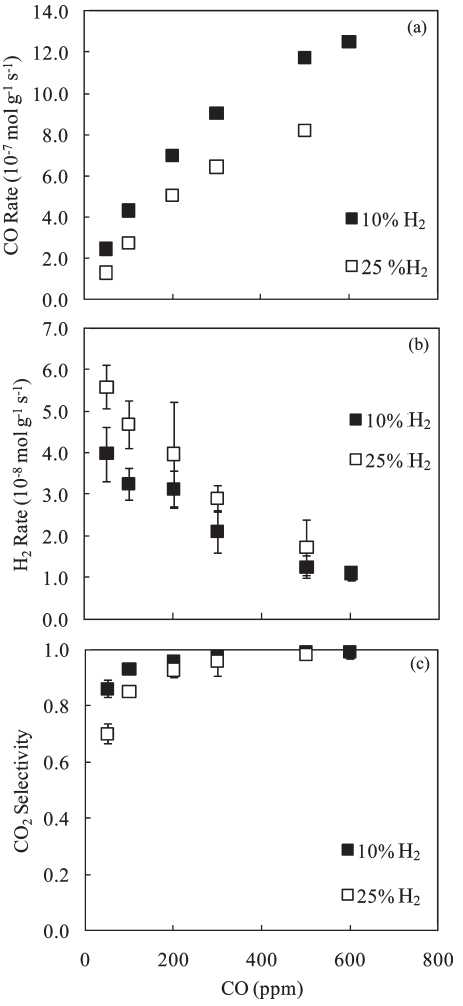

Figure 1. CO rate (a), H_2 rate (b), and CO_2 selectivity (c) as a function of CO partial pressure during PROX over CuO_x-CeO_2 at 353 K (stoichiometric CO and O_2, 10% or 25% H_2, 150 sccm; 90% confidence intervals on each CO and H_2 mean rate are calculated based on three measurements using a t-distribution; 90% confidence intervals on the selectivity were propagated from the rate errors).

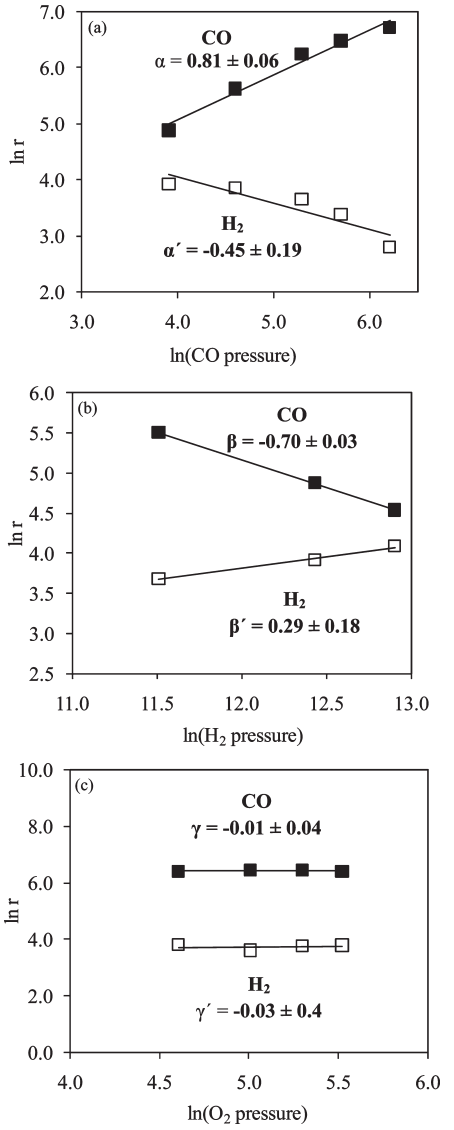

Figure 2. CO and H_2 oxidation orders over CuO_x-CeO_2 for (a) CO pressure (50−500 ppm CO, 200 ppm O_2, 25% H_2), (b) H_2 pressure (10−40% H_2, 50 ppm CO, 25 ppm O_2), and (c) O_2 pressure (10−250 ppm O_2, 25% H_2, 300 ppm CO) at 353 K, where $r_{CO} = k[H_2]^{\alpha}[CO]^{\beta}[O_2]^{\gamma}$ and $r_{H2} = k'[H_2]^{\alpha'}[CO]^{\beta'}[O_2]^{\gamma'}$; error is reported as a 90% confidence interval on the slope).

3.2. CO, H_2, and O_2 Reaction Orders at Low CO Concentrations. Figure 2 shows the CO and H_2 oxidation reaction rate dependence on CO, H_2, and O_2 pressures over CuO_x-CeO_2 and the resultant reaction orders at low CO and O_2 concentrations (50−500 ppm). CO rates were normalized to $r_0 = 10^{-7}$ mol g^{-1} s^{-1} and H_2 rates were normalized to $r_0 = 10^{-8}$ mol g^{-1} s^{-1} prior to the natural log function. All reaction orders measured are within the bounds expected from our previously proposed kinetic model describing a competitive adsorption mechanism between CO and H_2 on identical actives redox sites on the CuO_x-CeO_2 surface and are consistent with the higher CO and O_2 concentration measurements (CO: 0.5−4%; O_2: 0.25−1%; H_2: 5−100%) previously reported.[10] The error values of the reaction orders are calculated assuming that the random samples follow a t-distribution, which was used to calculate 90% confidence intervals on the slope parameter.

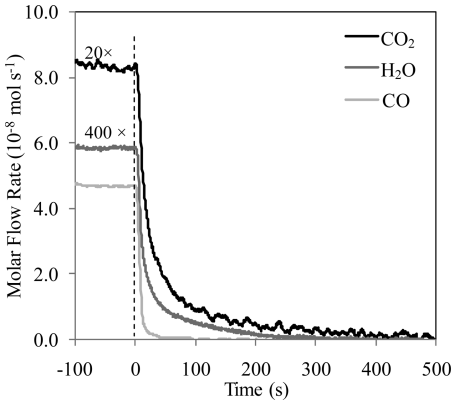

Figure 3. Molar flow rates of CO, CO_2, and H_2O after removal of either CO or H_2 reactants from the feed stream. (Steady state reaction conditions at $t < 0$: 500 ppm CO, 250 ppm O_2, 25% H_2, balance He, 150 sccm, 353 K).

3.3. Quantitative Analysis by the Reactive Titration Method. During preferential oxidation of CO in H_2, both CO and H_2 adsorb on the surface of CuO_x-CeO_2 and are oxidized to CO_2 and H_2O via a Mars and van Krevelen redox mechanism.[10] The CO molecules that adsorb on the surface during the PROX reaction and subsequently oxidize and leave the surface as CO_2 are denoted as reactive CO and are quantified by tracking CO_2 amounts. The CO molecules that adsorb on the surface during PROX but simply desorb as CO are denoted as unreactive CO and are quantified by tracking CO amounts (after some corrections as described below). Similarly, H_2 molecules that adsorb on the surface during PROX and oxidize to H_2O are denoted as reactive H_2 and are quantified by tracking H_2O formation. Figure 3 shows the molar flow rates of CO_2 and CO during an oxidative reaction with CO and H_2 at steady state ($t < 0$) and after removing CO from the reaction feed stream (at $t = 0$). Figure 3 also shows the molar flow rate of H_2O during a separate steady state reaction with CO and H_2 before ($t < 0$) and after removing H_2 from the feed stream (at $t = 0$).

The molar amounts of reactive CO and H_2 were calculated by integrating the area under the CO_2 and H_2O curves, respectively. The total amount of unreactive CO leaving the reactor during the titration event (A_T) is obtained by integrating the molar flow rate of CO over time. This amount includes CO adsorbed on the catalyst surface that does not oxidize to CO_2 on active sites, CO adsorbed on the inert SiO_2 diluent, and CO present in the gas phase. To accurately obtain the amount of unreactive CO adsorbed on the CuO_x-CeO_2 catalyst surface (A_1), the same measurement was carried out at the same conditions using (1) an empty reactor (no catalyst or SiO_2) to obtain the amount of gas phase CO (A_2) exiting the reactor over the same time period and (2) a reactor with only SiO_2 (no catalyst) to obtain the combined amount of gas phase CO and unreactive CO adsorbed on SiO_2 (A_3). Then the amount of unreactive CO adsorbed on the catalyst was calculated as: $A_1 = A_T - A_2 - (A_3 - A_2)$. As shown in Table 1, the amount of unreactive CO adsorbed on SiO_2 is less than 4% of the amount adsorbed on the CuO_x-CeO_2 catalyst at all conditions investigated. Three runs were performed for each CO pressure, and the values reported in Table 1 represent the sample mean.

3.4. Quantitative Analysis by the SSITKA Method. SSITKA was used to quantify the amount of adsorbed reactive CO for

dx.doi.org/10.1021/cs200037g |ACS Catal. 2011, 1, 519–525

Table 1. Molar Amounts of Unreactive CO Adsorbed on the CuO_x-CeO_2 Catalyst and the Inert SiO_2 Diluent during PROX at 353 K

	unreactive CO on SiO_2 (10^{-7} mol g^{-1})		unreactive CO on CuO_x-CeO_2 (10^{-7} mol g^{-1})			
	reactive titration		reactive titration		SSITKA	
CO (ppm)	10% H_2	25% H_2	10% H_2	25% H_2	10% H_2	25% H_2
50	0.3	0.3	7.0	6.0		
100	0.7	0.4	19.4	9.7	3.8	3.8
200	2.0	0.5	58.7	26.3		13.3
300	1.9	1.0	63.7	49.2		
500	2.8	1.1	77.2	63.2		
600	3.1		102.2		32.5	

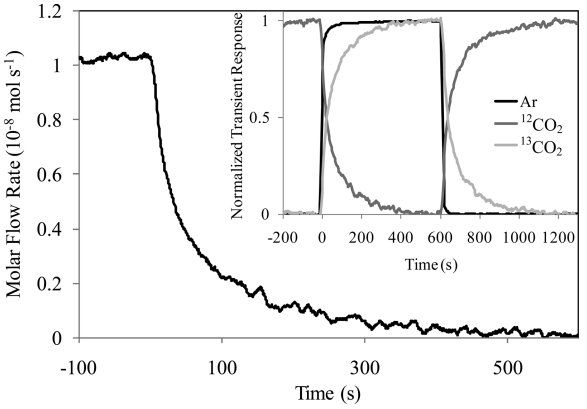

Figure 4. Molar flow rate of $^{12}CO_2$ during an isotope switch from ^{12}CO to ^{13}CO/Ar. The inset shows the normalized molar flow rates of $^{12}CO_2$, $^{13}CO_2$, and Ar during the isotopic switch. (Steady state reaction conditions: $t < 0$: 600 ppm ^{12}CO; $0 < t < 600$ s: 600 ppm ^{13}CO; and $t > 600$ s: 600 ppm ^{12}CO (all with 300 ppm O_2, 10% H_2, balance He, 150 sccm, 353 K).

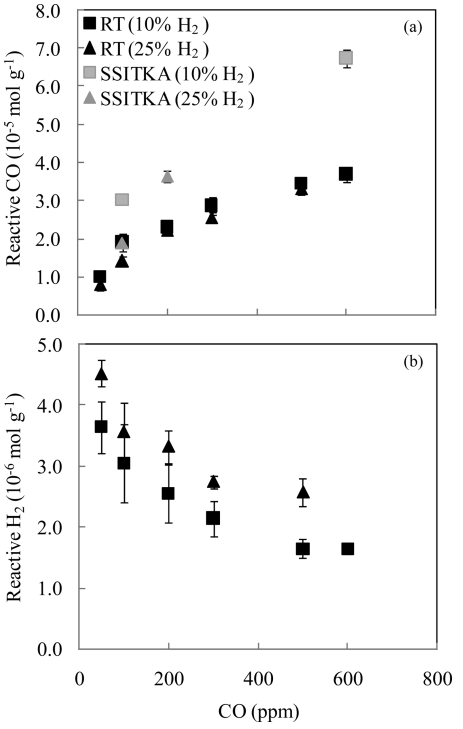

Figure 5. Molar amounts of reactive CO (a) and reactive H_2 (b) during PROX on CuO_x-CeO_2 as a function of CO partial pressure. Reactive CO is measured using both reactive titration (RT) and SSTIKA methods, and reactive H_2 is measured using the RT method. (stoichiometric CO and O_2, 10% and 25% H_2, 150 sccm, 353 K; error bars represent 90% confidence intervals on the mean based on three experiments).

comparison with that obtained using the reactive titration method. Unlike the reactive titration method, reactant and product concentrations, along with flow rates, remain undisturbed during the isotope switch from ^{12}CO to ^{13}CO. Thus analysis of the steady-state kinetic behavior of the catalyst surface is rigorous. The one failure of the reactive titration method is that the CO gas pressure is diminishing with time during the titration, and as detailed previously, the CO oxidation rate over CuO_x-CeO_2 markedly depends on CO pressure. From this comparative study using dual methods, we will explore influences from the gas phase CO pressure on measured surface coverages and identify any limitations from the reactive titration method.

The molar amount of reactive ^{12}CO, measured by the isotope switch experiment, is calculated by integrating the area under the $^{12}CO_2$ curve after a ^{12}CO to ^{13}CO/Ar switch (Figure 4). The inset in Figure 4 shows the normalized molar flow rates of $^{12}CO_2$, $^{13}CO_2$, and Ar at steady-state ($t < 0$), after the isotope switch from ^{12}CO to ^{13}CO/Ar ($0 \leq t < 600$ s), and after the reverse isotope switch from ^{13}CO/Ar to ^{12}CO ($t > 600$ s). Upon both switches, $^{12}CO_2$ and $^{13}CO_2$ curves show a mirror-image of each other and cross at 0.5 of the normalized transient response, as desired.

3.5. Effect of CO Pressure on Molar Amounts of Reactive CO, Unreactive CO, and Reactive H_2. The molar amounts of CO that adsorbs and oxidizes to CO_2 (reactive CO) and of H_2 that adsorbs and oxidizes to H_2O (reactive H_2), measured using the reactive titration method and SSITKA, are shown in Figures 5a and 5b, respectively, as a function of the CO pressure in the reactant feed during PROX at 353 K. The molar amount of reactive CO increases sharply with increasing CO pressure (Figure 5a) in both 10% H_2 and 25% H_2, but is in all cases lower at the larger H_2 concentration. The amount of unreactive CO on the surface increases only slightly with increasing CO pressure and is also reduced by the presence of 25% H_2 relative to 10% H_2, as previously shown in Table 1. Because of the small amount of unreactive H_2 adsorbed on CuO_x-CeO_2 compared with the gas phase H_2, the unreactive H_2 amount is not reported here. The

dx.doi.org/10.1021/cs200037g |ACS Catal. 2011, 1, 519–525

amount of reactive CO is higher than that of unreactive CO at every CO pressure, with the disparity increasing at higher CO pressures, indicating that the majority of CO is adsorbed on active redox sites capable of oxidizing CO at 353 K. The amount of reactive H_2 on the surface during PROX decreases with increasing CO pressure and is larger at 25% H_2 relative to 10% H_2 as shown in Figure 5b. An increase in the amount of H_2 adsorbed on the catalyst surface and oxidized to H_2O is observed with an increase of H_2 pressure or a decrease of CO pressure in the gas phase. CO adsorption clearly inhibits H_2 adsorption and reaction, and thus CO coverage is a vital determiner for CO oxidation selectivity. At CO concentrations below 400 ppm, many reactive sites remain vacant (not yet saturated by CO) and either H_2 or CO can adsorb. However, as the CO concentration increases in this range, the coverage of reactive and unreactive CO increases markedly (as shown in Table 1 and Figure 5a). The increasing presence of adsorbed CO decreases the probability of H_2 adsorbing on the surface. At higher CO pressures, CO saturation leads to 100% CO_2 selectivity while preventing reactive adsorption of H_2. The final influence of this competitive adsorption is that the H_2 oxidation rate (per g of catalyst) decreases with increasing CO pressure (Figure 1) because of the change in coverage at these conditions.

The molar amount of reactive CO measured by SSITKA (Figure 5a) is marginally higher than that measured by reactive titration method at each CO pressure investigated, with a larger disparity observed at 600 ppm CO. Furthermore, the amounts of unreactive CO adsorbed on the CuO_x-CeO_2 catalyst measured by the SSITKA method are slightly lower than those measured by reactive titration at identical CO feed pressures (Table 1). Although more expensive to perform, isotope switch results should be more accurate because of the constant CO feed pressure, which will retain all surface species during titration and capture the true steady-state reaction conditions. Molar surface amounts measured using the SSITKA method are thus slightly larger because, with the higher gas phase CO pressure, more CO adsorbs and reacts over the time period of the titration event. This is also consistent with smaller molar amounts of unreactive CO measured using the SSITKA method; an increase in CO pressure in the gas phase promotes CO oxidation rather than desorption.

3.6. Effect of O_2 Pressure on Molar Amounts of Reactive CO and on Oxidation Rates. Polster et al. previously reported that neither CO nor H_2 rates are dependent on O_2 pressure at relatively high partial pressures (0.25%−1%).[10] Figure 6a and 6b show that the CO rate, H_2 rate, and CO_2 selectivity also are not dependent on O_2 concentration at low O_2 pressures (50−250 ppm). It is often proposed that CO and H_2 oxidation over copper ceria follows the Mars and van Krevelen pathway through the facile synergistic redox cycles between the active copper and the support (Ce^{4+}-O^{2-}-Cu^{2+} ↔ Ce^{3+}-□-Cu^{+}).[4,27−30] As long as the oxygen supply is prevalent to reoxidize the surface in a kinetically irrelevant step, rates are independent of O_2 pressure;[1,31,32] however, as the oxygen pressure approaches zero, both CO and H_2 rates become dependent on O_2 pressure if reoxidation is rate limiting.

Figure 6c shows that the amount of reactive CO on the surface, measured by reactive titration, is constant with O_2 concentration from 100 to 250 ppm O_2. Apart from the independence of CO rate on O_2 partial pressure, this shows that excess gas phase oxygen does not compete with CO adsorption in any way that may affect CO adsorption and oxidation on active redox sites.

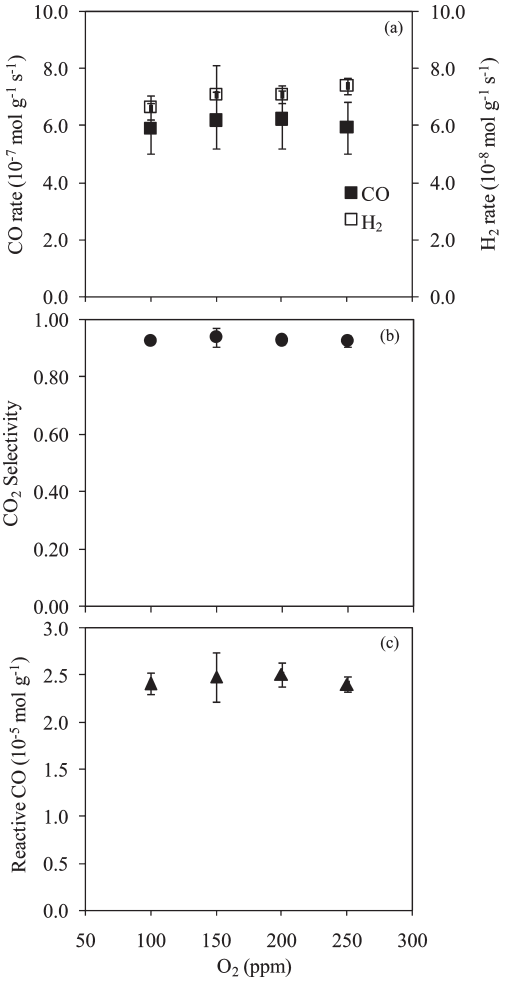

Figure 6. CO and H_2 rates (a), CO_2 selectivity (b), and reactive CO amounts (c) on CuO_x-CeO_2 as a function of O_2 partial pressure during PROX (300 ppm CO, 100−250 ppm O_2, 25% H_2, 150 sccm, 353 K; error bars represent 90% confidence intervals on the mean based on three experiments).

3.7. CO_2 Selectivity versus CO Coverage. To better describe the competitive reaction mechanism between CO and H_2 over CuO_x-CeO_2, and its impact on CO_2 selectivity, two coverage models were investigated for the purpose of correlating CO_2 selectivity with CO coverage using the previously described molar amounts of reactive CO and H_2. In model 1, the reactive CO coverage is defined as the ratio of the reactive CO amount at a given CO pressure to the reactive CO amount at 600 ppm CO (eq 1). With 600 ppm CO in the feed, the CO_2 selectivity reaches 100%; thus, the reactive CO amount at this condition is used as an estimate of the total number of active redox sites for either CO or H_2 in this model. In other words, the assumption is that at 600 ppm, the 100% CO oxidation selectivity is attained because only CO adsorbs on redox sites; thus active sites are presumed to become saturated with CO at this pressure in preference over H_2. Similarly, the reactive H_2 coverage is defined as the ratio of the reactive H_2 amount at a given CO pressure to the reactive CO amount at 600 ppm CO (eq 2). If CO and H_2 follow a true competitive adsorption and reaction mechanism on the same active sites, these sites should be equally accessible to both CO and H_2, and equally capable of oxidizing CO and H_2 at all CO pressures after adsorption (dissociative adsorption for H_2). For

dx.doi.org/10.1021/cs200037g |ACS Catal. 2011, 1, 519–525

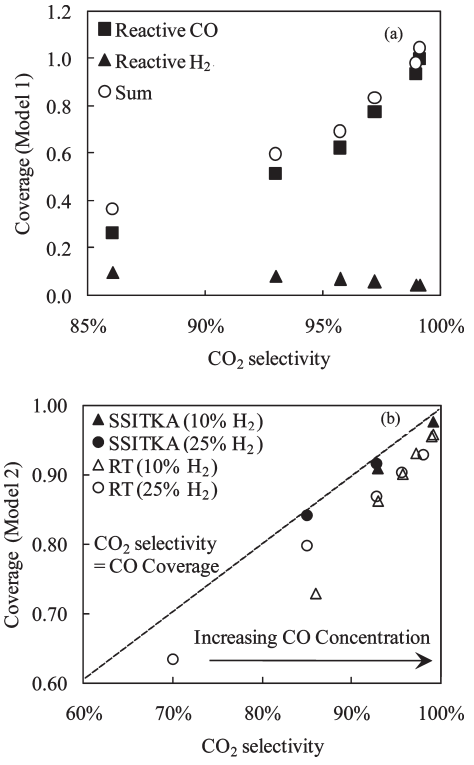

Figure 7. CO_2 selectivity correlation with (a) reactive CO and H_2 coverages using coverage Model 1 relative to the reactive CO adsorbed at 600 ppm CO by reactive titration (stoichiometric CO and O_2, 25% H_2, 150 sccm, 353 K), and (b) reactive CO coverage using coverage Model 2 relative to the reactive CO and H_2 adsorbed at the same CO pressure by reactive titration (RT) and SSITKA (stoichiometric CO and O_2, 10% and 25% H_2, 150 sccm, 353 K).

this model to be sufficiently descriptive, the reactive CO coverage and the reactive H_2 coverage should sum to 1, since CO oxidation selectivity loss is due to the adsorption and oxidation of H_2 over the same active sites at lower CO pressures where CO does not saturate all redox sites.

$$\theta_{\text{CO-model 1}} = \frac{\text{Reactive CO amount } (\times \text{ ppmCO})}{\text{Reactive CO amount } (600 \text{ ppmCO})} \quad (1)$$

$$\theta_{\text{H}_2\text{-model 1}} = \frac{\text{Reactive H}_2 \text{ amount } (\times \text{ ppmCO})}{\text{Reactive CO amount } (600 \text{ ppmCO})} \quad (2)$$

$$\theta_{\text{CO-model 2}} = \frac{\text{Reactive CO amount } (\times \text{ ppmCO})}{\text{Reactive CO amount } (\times \text{ ppmCO}) + \text{Reactive H}_2\text{amount } (\times \text{ ppmCO})} \quad (3)$$

Figure 7a shows reactive CO and H_2 coverage values based on Model 1 and using surface amounts measured from the reactive titration method as a function of CO pressure, along with their summation. Both the reactive CO coverage and the summation strongly increase with increasing CO pressure, with the summation only approaching 1 as the coverage approaches 1. Therefore, it is not accurate to assume that the active redox sites can equally oxidize CO and H_2 upon adsorption. As shown in Figure 7a, 86% CO_2 selectivity is achieved with a reactive CO coverage of only 28% and a reactive H_2 coverage of 11%. On the basis of this first competitive adsorption model and these coverage values, we expect the CO_2 selectivity to be 72% (calculated as $0.28/(0.28 + 0.11) \times 100\%$). However, selectivity is substantially larger than this and reflects the higher rate of CO oxidation relative to H_2 oxidation (Figure 1). Moreover, since the reactive H_2 coverage is observed to remain low (relative to CO) at all CO pressures, it is clear that the oxidized active sites (Cu−O*-Ce) are not as proficient at either dissociating or oxidizing H_2 at 353 K. This infers that CO oxidation is kinetically preferred over CuO_x-CeO_2 under the reaction condition presented.

Much of the inacuracy in Model 1 arises from neglecting the effect of CO pressure on the amount of reactive CO adsorbed as detailed in Figure 5a. Thus, in Model 2, CO coverage is defined as the ratio of the reactive CO amount at a given CO pressure to the sum of the reactive CO and H_2 amounts under at the same CO pressure (eq 3). For this model, coverages are reported using reactive CO amounts quantified by both the reactive titration method and the SSITKA method. Using this model, the reactive CO coverage dependence on PROX selectivity is shown in Figure 7b. If the reactive CO coverage is the only parameter controlling CO_2 selectivity, then CO_2 selectivity should show a one to one linear dependence on reactive CO coverage (indicated by the dotted line in Figure 7b). As observed, the CO coverage values, quantified by SSITKA, nearly match the corresponding CO_2 selectivity. Thus, this model confirms that the very high selectivity achievable over CuO_x-CeO_2 arises from a competitive redox mechanism of CO and H_2 over the same active sites, with the relative coverages of CO and H_2 controlling the CO_2 selectivity. Coverages calculated using reactive CO and H_2 amounts measured by reactive titration also validate this model. These values are slightly lower than the corresponding values measured using the expensive SSITKA method; however, general trends and coverage models can still be assessed using this inexpensive quantification method in certain cases. Validation using isotopes, however, is recommended for accuracy.

4. CONCLUSIONS

Through a combined study using both the reactive titration method and the steady-state isotopic-transient kinetic analysis, quantities of reactive CO and H_2 on the surface of CuO_x-CeO_2 during steady state CO PROX in excess H_2 were measured. The reactive titration method was introduced as an inexpensive protocol for measuring molar amounts of reactive CO, unreactive CO, and reactive H_2. It is shown that CO adsorption inhibits H_2 adsorption and reaction and vice versa. By defining reactive CO coverage as the ratio of the reactive CO amount at a given CO pressure to the sum of the reactive CO and H_2 amounts at the same CO pressure, the one-to-one linear dependence of CO_2 selectivity on reactive CO coverage indicates that relative CO and H_2 coverage is the determiner of CO_2 selectivity. Therefore, the high CO_2 selectivity achievable over CuO_x-CeO_2 arises from a competitive redox mechanism over the same active sites. The coverage model and general trends of adsorbed molar amounts can be assessed using the inexpensive reactive titration method in certain cases. Validation using SSITKA, however, is recommended for accurracy.

AUTHOR INFORMATION

Corresponding Author

*E-mail: baertsch@ecn.purdue.edu. Phone: (765) 496-7826. Fax: (765) 494-0805.

■ ACKNOWLEDGMENT

This work was supported by NSF (CBET Career Award #0644707).

■ REFERENCES

(1) Snytnikov, P. V.; Popova, W. M. M.; Men, Y.; Rebrov, E. V.; Kolb, G.; Hessel, V.; Schouten, J. C.; Sobyanin, V. A. *Appl. Catal., A* **2008**, *350*, 53–62.
(2) Gamarra, D.; Belver, C.; Fernández-García, M.; Martínez-Arias, A. *J. Am. Chem. Soc.* **2007**, *129*, 12064–12065.
(3) Gamarra, D.; Martínez-Arias, A. *J. Catal.* **2009**, *263*, 189–195.
(4) Caputo, T.; Lisi, L.; Pirone, R.; Russo, G. *Appl. Catal., A* **2008**, *348*, 42–53.
(5) Gamarra, D.; Munuera, G.; Hungría, A. B.; Fernández-García, M.; Conesa, J. C.; Midgley, P. A.; Wang, X. Q.; Hanson, J. C.; Rodríguez, J. A.; Martínez-Arias, A. *J. Phys. Chem. C* **2007**, *111*, 11026–11038.
(6) Polster, C. S.; Baertsch, C. D. *Chem. Commun.* **2008**, 4046–4048.
(7) López, I.; Valdés-Solís, T.; Marbán, G. *Int. J. Hydrogen Energy* **2008**, *33*, 197–205.
(8) Marbán, G.; Fuerte, A. B. *Appl. Catal., B* **2005**, *57*, 43–53.
(9) Gómez-Cortés, A.; Márquez, Y.; Arenas-Alatorre, J.; Díaz, G. *Catal. Today* **2008**, *133−135*, 743–749.
(10) Polster, C. S.; Nair, H.; Baertsch, C. D. *J. Catal.* **2009**, *266*, 308–319.
(11) Martínez-Arias, A.; Hungría, A. B.; Munuera, G.; Gamarra, D. *Appl. Catal., B* **2006**, *65*, 207–216.
(12) Martínez-Arias, A.; Gamarra, D.; Fernández-García, M.; Wang, X. Q.; Hanson, J. C.; Rodriguez, J. A. *J. Catal.* **2006**, *240*, 1–7.
(13) Liu, W.; Flytzani-Stephanopoulos, M. *J. Catal.* **1995**, *153*, 317–332.
(14) Liu, W.; Sarofim, A. F.; Flytzani-Stephanopoulos, M. *Chem. Eng. Sci.* **1994**, *49*, 4871–4888.
(15) Liu, W.; Flytzani-Stephanopoulos, M. *Chem. Eng. J.* **1996**, *64*, 283–294.
(16) Sedmak, G.; Hočevar, S.; Levec, J. *J. Catal.* **2003**, *213*, 135–150.
(17) Luo, M.-F.; Song, Y.-P.; Lu, J.-Q.; Wang, X.-Y.; Pu, Z.-Y. *J. Phys. Chem. C* **2007**, *111*, 12686–12692.
(18) Skårman, B.; Grandjean, D.; Benfield, R. E.; Hinz, A.; Andersson, A.; Wallenberg, L. R. *J. Catal.* **2002**, *211*, 119–133.
(19) Luo, F.; Ma, J.-M.; Lu, J.-Q.; Song, Y.-P.; Wang, Y.-J. *J. Catal.* **2007**, *246*, 52–59.
(20) Wang, J. B.; Lin, S.-C.; Huang, T.-J. *Appl. Catal., A* **2002**, *232*, 107–120.
(21) Zeradine, S.; Bourane, A.; Bianchi, D. *J. Phys. Chem. B* **2001**, *105*, 7254–7257.
(22) Bourane, A.; Dulaurent, O.; Bianchi, D. *J. Catal.* **2000**, *195*, 406–411.
(23) Shannon, S. L.; Goodwin, J. G., Jr. *Chem. Rev.* **1995**, *95*, 677–695.
(24) Savva, P. G.; Efstathiou, A. M. *J. Catal.* **2008**, *257*, 324–333.
(25) Pansare, S. S.; Sirijaruphan, A.; Goodwin, J. G., Jr. *J. Catal.* **2005**, *234*, 151–160.
(26) Rothaemel, M.; Hanssena, K. F.; Blekkana, E. A.; Schanke, D.; Holmen, A. *Catal. Today* **1998**, *40*, 171–179.
(27) Wang, S.-P.; Zhang, T.-Y.; Su, Y.; Wang, S.-R.; Zhang, S.-M.; Zhu, B.-L.; Wu, S.-H. *Catal. Lett.* **2008**, *121*, 70–76.
(28) Cao, J.-L.; Wang, Y.; Zhang, T.-Y.; Wu, S.-H.; Yuan, Z.-Y. *Appl. Catal., B* **2008**, *78*, 120–128.
(29) Sirichaiprasert, K.; Luengnaruemitchai, A.; Pongstabodee, S. *Int. J. Hydrogen Energy* **2007**, *32*, 915–926.
(30) Wang, X.; Rodriguez, J. A.; Hanson, J. C.; Gamarra, D.; Martínez-Arias, A.; Fernández-García, M. *J. Phys. Chem. B* **2005**, *109*, 19595–19603.
(31) Ayastuy, J. L.; Gurbani, A.; González-Marcos, M. P.; Gutiérrez-Ortiz, M. A. *Ind. Eng. Chem. Res.* **2009**, *48*, 5633–5641.
(32) Lee, H. C.; Kim, D. H. *Catal. Today* **2008**, *132*, 109–116.